PHYSICAL REVIEW E VOLUME 60, NUMBER 2 AUGUST 1999

Intrinsic localized modes and chaos in damped driven rotator lattices

D. Bonart* and J. B. Page
Department of Physics and Astronomy, Arizona State University, Tempe, Arizona 85287-1504
(Received 28 May 1998; revised manuscript received 27 May 1999)

It is shown that intrinsic localized rotational modes (ILRMs) in parametrically driven damped lattices of coupled classical dipole rotators can become chaotic without losing their localized character. Insight into this behavior is obtained by means of a nonlinear stability analysis. Moreover, we discuss a robust scheme for exploiting a spatially extended chaotic state to generate stationary randomly spaced arrays of driven ILRMs, and show that the associated absorption exhibits unusual signatures. [S1063-651X(99)51308-1]

PACS number(s): 05.45.−a, 63.20.Ry, 63.20.Pw, 78.20.Bh

While vibrational intrinsic localized modes (ILMs) arising from nonlinearity in periodic lattices are by now well understood theoretically [1], they have yet to be verified in the laboratory. Here, we discuss dynamical features of intrinsic localized rotational modes (ILRMs) in lattices of coupled rotators, which give promising directions for filling this gap. Our model represents a simplified view of dipolar molecules with orientational degrees of freedom which are adsorbed on crystal surfaces (see, e.g., [2]) or occur in crystals such as KCN [3]. Josephson junction ladders [4] also fit into this scheme, although here we will treat the rotators as optically driven electric dipoles. Atomic scale localized dynamical structures at surfaces may be of technological interest in the context of high temperature catalytic processes or high density memory units.

ILRMs are stationary solutions of the coupled nonlinear classical equations of motion and consist of a rotational center comprising one or few rotating dipoles plus librational wings. ILRMs in undriven lattices were proposed recently by Takeno and Peyrard [5]. However, real systems exhibit damping, so that external driving is needed to sustain stationary modes. Hence, our focus is on continuously driven and damped lattices. In contrast to the recently discussed case of transient optical excitation of vibrational ILMs [6], we will see that the richer dynamics of driven rotator lattices leads to a robust scheme for both creating and detecting ILRMs, within the simpler case of continuous optical driving. This is achieved by exploiting the existence of a regime of spatially extended chaotic response. We will also discuss a different regime where the system exhibits an interesting *localized* chaotic response. While aspects of chaos in systems with one or a few rotators have been discussed in the literature (see, e.g., [7]), ILRM-type excitations in lattices were not included. Our concern is dynamical behavior that combines both phenomena.

Here we discuss a one-dimensional (1D) lattice of identical dipoles with one orientational degree of freedom θ_l per site l, although we have generalized our work to unrestricted rotations and higher dimensions [8]. After rescaling the time to eliminate the dipoles' moment of inertia, we obtain the equations of motion in the dimensionless form

$$-\ddot{\theta}_l = o_2 \sin(\theta_l) + f_l(t) + \gamma\dot{\theta}_l + k_2 \sum_{l'=l\pm1} [-\sin(\theta_l - \theta_{l'}) + 3\cos(\theta_l)\sin(\theta_{l'})]. \quad (1)$$

Here o_2 denotes the strength of a hindering potential modeling, e.g., an adsorbate-substrate coupling, γ is the linear damping constant, and k_2 is the strength of nearest-neighbor (NN) dipole-dipole coupling. The lattice is oriented along z, with the dipoles rotating in the xz plane. The driving force $f(t)$ is parametric for the case of dipoles coupled to an external electric field $f_l(t) = f_d \cos(\omega_d t)\sin(\theta_l)$, and it is nonparametric for an ac-driven Josephson ladder. We focus here on the parametric driving case. Our parameter values are $k_2 = 0.1$, $o_2 = 1$, $f_d = 1$, and $\gamma = 0.1$.

Stationary solutions are efficiently obtained by invoking an extended rotating-wave approximation (RWA). We include frequencies ranging from the first subharmonic of the driving frequency (to describe the primary librational response) through the second harmonic (needed for the free-rotor limit). Thus we take

$$\theta_l(t) = \omega_d t \kappa_l - \tau_l + \sum_{n=1}^{4} [u_l^{(n)} \sin(n\omega_d t/2) + v_l^{(n)} \cos(n\omega_d t/2)], \quad (2)$$

where κ_l is fixed at 1 for rotational motion and is zero for librations. After substituting this into Eq. (1), we project out equations for τ_l, $u_l^{(n)}$, and $v_l^{(n)}$ by multiplying by 1, $\sin(\omega_d t/2)$, $\cos(\omega_d t/2)$, etc. and numerically integrating over two driving periods $4\pi/\omega_d$. The resulting set of coupled nonlinear equations is solved using standard numerical methods, and the predictions are verified by molecular dynamics (MD).

The relevance of a stationary solution $\underline{z}(t) \equiv [\theta_1(t), \theta_2(t), \ldots, \dot{\theta}_1(t), \dot{\theta}_2(t), \ldots]$ obtained this way depends crucially on its dynamical stability. The Floquet stability analysis is based on the linearized equations of motion for perturbations $\delta\underline{z}(t)$ of the stationary mode. Following Ref. [9], we set up the linear mapping $\delta\underline{z}(t+T) = \underline{M} \cdot \delta\underline{z}(t)$, where T is the predicted mode period. If the matrix $\underline{M}$ has any eigenvalues λ_j with $|\lambda_j| > 1$, $\underline{z}(t)$ is

*Present address: Infineon Technologies, Munich, Germany.

unstable; otherwise, it is stable. Beyond the linear regime, the perturbation eigenvectors $\{\underline{\chi}_j\}$ of $\underline{M}$ are useful for analyzing *nonlinear* instability. We monitor the strobed difference between the mode's actual trajectory, obtained in an MD simulation, and its predicted RWA trajectory, in terms of the eigenvectors,

$$\underline{z}_{\mathrm{MD}}(nT)-\underline{z}_{\mathrm{RWA}}(nT)=\sum_j a_j^n \underline{\chi}_j . \tag{3}$$

The amplitudes a_j^n are not only convenient for simple verification of predicted instability growth rates in the linear regime, but they also provide important insights into complex nonlinear instabilities, as will be seen below in our discussion of localized chaos.

The simplest types of response for an isolated driven dipole comprise zero response, librational response at $\omega_d/2$, and rotation at ω_d. For a lattice, we find stable ILRMs over a range of driving frequencies. These modes consist of a rotational center at ω_d, accompanied by either spatially decaying librational wings at ω_d or by nondecaying librational wings at $\omega_d/2$. Moreover, the rotational centers can involve several adjacent sites, without qualitatively altering the stability properties. For clarity, we first discuss ILRMs having a single rotating dipole.

For large driving frequencies ($\omega_d \gg 2.9$) we find ILRMs that closely resemble the undriven modes discussed in Ref. [5], i.e., having a rotational center and spatially decaying wings, all at ω_d. However, the external force causes these modes to occur in pairs consisting of one stable and one unstable solution, differing mainly by the phase of their rotational centers. We begin with the stable ILRM for $\omega_d=3$, slowly decrease ω_d in our MD simulation, and monitor the rescaled period-average kinetic energy at each site l,

$$\rho_l(t)=\frac{1}{\omega_d^2 T_d}\int_t^{t+T_d}\dot{\theta}_l^2 dt, \tag{4}$$

where $T_d=2\pi/\omega_d$ is the driving period. Note that $\rho_l(t)\approx 1$ for rotational motion, while $\rho_l(t)<1$ for librations. Figure 1 surveys some results. When the frequency $\omega_d \approx 2.85$ is reached, the ILRM spontaneously develops a spatially extended, subharmonic librational background of acoustic character, i.e., the background dipoles librate in phase. Further decrease of ω_d to ≈ 2.48 leads to an additional subharmonic bifurcation, and finally after a Hopf-bifurcation (see, e.g., Ref. [14]) to a range of chaotic response ($\omega_d \approx 2.38,\ldots,2.41$), which has an interesting nature.

First, we notice in Fig. 1 that the chaotic spread in phase space decreases with increasing distance from the mode's rotational center; the chaos is localized. Second, the mode's time trajectories $\{\dot{\theta}_l(t)\}$ (not given here) reveal two timescales. The first corresponds to the driving period T_d, and the trajectories appear nonchaotic on this timescale. However, on a larger time scale ($\sim 100T_d$ at $\omega_d=2.4$), we find that the envelopes of the trajectories exhibit a chaotic ''pulsing,'' whose details are sensitive to small changes of ω_d. Insight is provided by the expansion of Eq. (3), using the Floquet eigenvectors for the unstable RWA-predicted ILRM. Results for $\omega_d=2.4$ are given in Fig. 2, which shows that

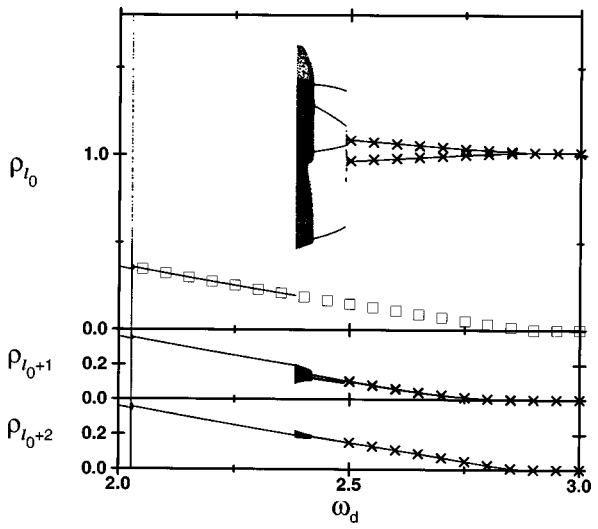

FIG. 1. Bifurcation diagrams for the period-average kinetic energy ρ_l at the rotational center l_0 and its first and second neighbors, for an ILRM in a periodic ten-dipole lattice. The MD simulation was begun for the stable RWA solution at $\omega_d=3$, and after 1000 cycles of the driving field, ρ_l was plotted for the next 500 cycles (thin dots). The frequency was then lowered by 0.001, and the process repeated. Also shown are the RWA predictions for stable ILRMs ($\times$) and for stable, spatially extended, subharmonic acoustic librational modes ($\square$) (upper panel only). For clarity, the figure does not include several other stable and unstable predicted stationary solutions.

only two of the perturbation eigenvectors gain appreciable amplitudes with time. These are an instability eigenvector $\underline{\chi}_1$ with eigenvalue $|\lambda_1|>1$ (denoted as the *primary* instability) and its associated ''quasisymplectic'' partner $\underline{\chi}_2$ with $\lambda_2=\exp(-\gamma T)/\lambda_1$ (*secondary* instability). Both $\underline{\chi}_1$ and $\underline{\chi}_2$ are well localized, and they become strongly coupled anharmonically as the instabilities grow in time. It is this interplay which leads to the localized chaos: after the initial exponential growth phase of the primary instability it begins driving the secondary instability. As the secondary instability

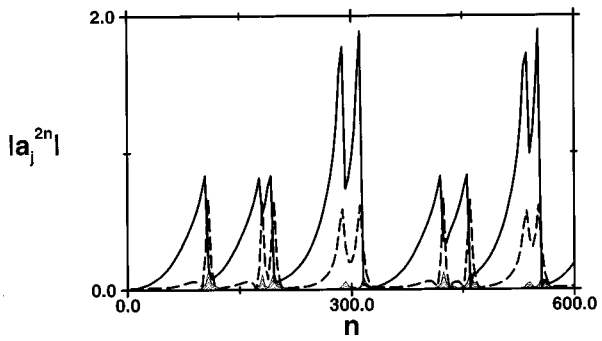

FIG. 2. Amplitude moduli $|a_i^{2n}|$ from the stability eigenvector description [Eq. (3)], applied to the finite time evolution of the unstable ILRM at $\omega_d=2.4$, in the lattice of Fig. 1. For clarity, we strobed the amplitudes at integer multiples of $4T_d$, i.e., twice the librational period, to eliminate fluctuations caused by the subharmonic nature of the primary instability (thick solid line). Only the primary instability and secondary instability (thick dashed line) acquire appreciable amplitudes, whereas those for all other eigenvectors (thin solid lines) remain small.

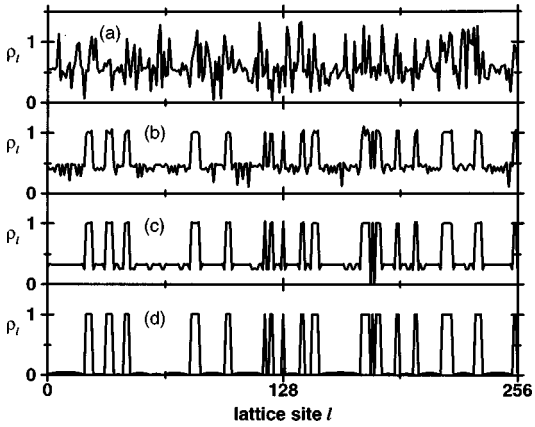

FIG. 3. Plots of ρ_l for the frequency ramping-up sequence applied to a 256-dipole lattice. The sequence starts at $\omega_d=2$, in the region of spatial-temporal chaotic response (Lyapunov exponent $=0.32$). The driving frequency is held at this value for 100 cycles, after which it is linearly increased by 0.002 per cycle. Shown are ρ_l for (a) $\omega_d=2.05$, (b) $\omega_d=2.30$, (c) $\omega_d=2.60$, and (d) $\omega_d=2.90$. As the frequency increases beyond the chaotic region, the librations and rotations ''decouple,'' and the librational response decreases. At large driving frequencies (d) the lattice is in a stationary state of randomly spaced ILRMs, between which the dipoles execute very small amplitude librations. The librations disappear at $\omega_d\approx 2.9$.

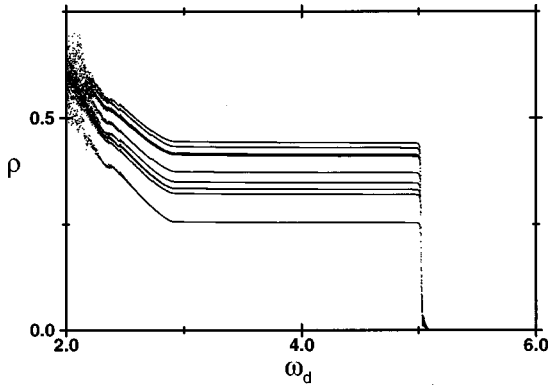

FIG. 4. Rescaled period-average absorption for the lattice of Fig. 3, for several ramping-up sequences. For each sequence, the frequency was ramped as described in Fig. 3, and owing to the spatial-temporal chaos at the initial time, the final ILRM array is different for each. The small features at $\omega_d\approx 2.3$ are due to an instability in the librating portions of the lattice.

becomes large, it ''switches off'' the primary instability and soon afterwards collapses as well. The system is then close to the initial conditions and the process begins again. The intervals between successive collapses of the primary instability are irregular, and Poincare sections prove that the behavior is indeed chaotic (Lyapunov exponent$=0.027$ at $\omega_d=2.4$). Note that the presence of dissipation in our system seems essential for localized chaos, since in the Hamiltonian case ($\gamma=0$), so-called Arnold diffusion should prevent localized chaos in general [10,11]. Note also that while the range of parameter space for these chaotic ILRMs is quite small, other types of local chaos have been discussed for various driven dissipative systems that do not involve intrinsic localized modes [12]. In view of those results and the chaotic ILRMs found here, we anticipate that driven chaotic ILMs should also exist in Josephson ladders [13] and damped driven lattice vibrational systems.

Decreasing ω_d further, we find that the localized chaotic attractor abruptly disappears at $\omega_d\approx 2.38$, due to a *boundary crisis* [14], in which the attractor crosses into another mode's basin of attraction and finally evolves into the stable, spatially extended, subharmonic acoustic librational mode. Continuing to decrease the driving frequency, we find that this mode becomes unstable at $\omega_d\approx 2.04$, below which it exhibits temporal and spatially extended chaos, which can be viewed as a mixture of librational and rotational motion. We now discuss how this chaotic response can be exploited to generate stable, nonchaotic ILRMs.

In MD, we begin driving a 256-dipole lattice in this chaotic regime at $\omega_d=2$, adding small random noise until the chaos has fully developed. We then slowly ramp up the driving frequency, and as we leave the range of chaotic response, we pick up rotational domains ($\rho_l\approx 1$) and subharmonic librational domains ($\rho_l<1$) from the chaotic state. This is seen in Fig. 3. As ω_d is increased, the librational response decreases to zero, resulting in a stationary, randomly spaced array of stable ILRMs, most of which are composed of several adjacent rotators. We have also used this generation scheme for 2D lattices of scalar coupled dipoles and for 1D and 2D dipole lattices with unrestricted 3D rotations [8]. The scheme proves to be very robust, leading in all cases to random arrays of ILRMs.

This technique for generating driven ILRMs from a chaotic state also provides a means for their detection, through several unusual features exhibited by the associated period-average power absorption. These are conveniently illustrated via the quantity $\rho\equiv 1/N\,\Sigma_l\rho_l$, where N is the total number of sites. For stationary response, ρ is proportional to the absorption divided by ω_d^2, and Fig. 4 plots $\rho(\omega_d)$ for several repetitions of the ramping-up sequence discussed above. First, because of the small random noise used to establish the initially chaotic response, each sequence produces a different absorption curve. All of the curves exhibit three characteristic regions: (a) a small, initially chaotic region, (b) a region of roughly linear decrease until the librational response disappears, and (c) a flat plateau ($\omega_d\approx 2.9,\ldots,4.9$) where, to a good approximation, the absorption of the created ILRM array varies as ω_d^2. The plateau heights directly reflect the number of rotating dipoles captured from the initially chaotic state. Finally, there is a cutoff at $\omega_d\approx 5$, beyond which the parametric drive cannot supply energy fast enough to sustain the rotational motion.

In summary, our study of optically driven and damped perfect lattices of rotating dipoles has revealed unusual and useful connections between intrinsic localized rotational modes and chaos. First we have shown that such modes may exhibit a long timescale chaotic behavior without losing their localized character. A stability perturbation eigenvector analysis of this mode's MD trajectories showed that the chaos stems from the dynamics of a pair of localized eigenvectors, which become strongly coupled anharmonically over extended times, but remain localized. Second, we have exploited the existence of a spatially extended chaotic regime to demonstrate a simple and robust scheme for optically generating ILRMs, by slowly increasing the driving frequency out of the chaotic regime. Third, we have shown

that monitoring the classical absorption during this process yields unusual signatures. These phenomena also carry over to higher-dimensional systems with unrestricted rotational degrees of freedom [8].

Our model and parameter values were chosen both to facilitate the MD simulations and to reveal interesting dynamical phenomena of coupled dipole rotator lattices. To treat candidate experimental systems, however, the inclusion of additional aspects, such as vibrational degrees of freedom and electronic polarizability will likely lead to even more complex dynamics. And while values of the damping constant could be computed perturbatively or estimated phenomenologically from observed lifetimes of small-angle librational transitions, the speculative quantum theory of vibrational local mode damping in Ref. [15] suggests that modifications of our assumed linear form may be necessary at high energies. Nevertheless, our results strongly suggest that in extensions to more sophisticated models, the interplay between chaos and intrinsic localized modes can play an important and practical role in the study of strongly anharmonic lattices.

This work was supported by the Alexander von Humboldt Foundation and NSF Grant No. DMR-9510182. We thank L. Floria for a preprint of his work.

[1] See, for instance, A. J. Sievers and J. B. Page, in *Dynamical Properties of Solids VII Phonon Physics*, edited by G. K. Horton and A. A. Maradudin (Elsevier, Amsterdam, 1995), p. 137; S. Flach and C. R. Willis, Phys. Rep. **295**, 181 (1998).

[2] Y. T. Shih, D. S. Chuu, and W. N. Mei, Phys. Rev. B **54**, 10 938 (1996).

[3] J. Ortiz-Lopez, M. Siu Li, and F. Luty, Phys. Status Solidi B **199**, 245 (1997).

[4] L. M. Floria, J. L. Marin, P. J. Martinez, F. Falo, and S. Aubry, Europhys. Lett. **36**, 539 (1996).

[5] S. Takeno and M. Peyrard, Physica D **92**, 140 (1996); Phys. Rev. E **55**, 1922 (1997).

[6] T. Rössler and J. B. Page, Phys. Rev. Lett. **78**, 1287 (1997).

[7] G. Benettin, L. Galgani, and A. Giorgilli, Nuovo Cimento B **89**, 103 (1985); E. J. Banning, J. P. van der Weele, J. C. Ross, M. M. Kettenis, and E. de Kleine, Physica A **245**, 11 (1997); D. D'Humieres, M. R. Beasley, B. A. Huberman, and A. Libchaber, Phys. Rev. A **26**, 3483 (1982); M. L. Rossi, M. Torri, and G. P. Brivio, Surf. Sci. **387**, 112 (1997).

[8] D. Bonart and J. B. Page (unpublished).

[9] K. W. Sandusky and J. B. Page, Phys. Rev. B **50**, 866 (1994).

[10] A. J. Lichtenberg and M. A. Liebermann, *Regular and Stochastic Motion* (Springer, New York, 1983).

[11] However, we have recently found a chaotic ILM for our rotator system in the absence of driving and damping. Numerical simulations show that this mode remains localized for at least 10^5 librational periods, indicating that Arnold diffusion is either extremely slow or is suppressed by numerical noise. The first paper in [7] also gives an example of localized chaos in a Hamiltonian lattice, but the issue of Arnold diffusion is not discussed.

[12] A. Greenfield, S. Putterman, and W. Wright, Phys. Lett. A **185**, 321 (1994); R. J. Deissler and H. R. Brand, Phys. Rev. Lett. **72**, 478 (1994); J. Kim, H. Park, and H. Moon, Phys. Rev. E **55**, 3948 (1997).

[13] After submission of this paper, we became aware of computer simulations of localized chaos in a *nonparametrically* driven Josephson ladder [P. J. Martinez, L. M. Floria, F. Falo, and J. J. Mazo, Europhys. Lett. **45**, 444 (1999)].

[14] E. Ott, *Chaos in Dynamical Systems* (Cambridge University Press, Cambridge, England, 1993).

[15] V. Hizhnyakov, Phys. Rev. B **53**, 13 981 (1996).